Available online at www.sciencedirect.com
ScienceDirect
Carbohydrate Research 342 (2007) 1895–1903
Carbohydrate RESEARCH

Structural transition of a 15 amino acid residue peptide induced by GM1

Naoki Fujitani,[a] Hiroki Shimizu,[b,*] Teruhiko Matsubara,[c] Takashi Ohta,[b] Yuuki Komata,[a] Nobuaki Miura,[a] Toshinori Sato[c] and Shin-Ichiro Nishimura[a,b,*]

[a]*Division of Advanced Chemical Biology, Graduate School of Advanced Life Science, Frontier Research Center for Post-Genomic Science and Technology, Hokkaido University, Sapporo 011-0021, Japan*
[b]*Drug-Seeds Discovery Research Laboratory, Hokkaido Center, National Institute of Advanced Industrial Science and Technology (AIST), Sapporo 062-8517, Japan*
[c]*Department of Biosciences and Informatics, Keio University, Yokohama 223-8522, Japan*

Received 16 February 2007; received in revised form 11 May 2007; accepted 15 May 2007
Available online 2 June 2007

Abstract—The ganglioside GM1-binding peptide, p3, with a sequence of VWRLLAPPFSNRLLP, displayed a clear structural alteration depending on the presence or absence of GM1 micelles. The three-dimensional structures of the p3 peptide in the free and GM1 bound states were analyzed using two-dimensional NMR spectroscopic experiments with distance-restrained simulated annealing calculations. The NMR experiments for the p3 peptide alone indicated that the peptide has two conformers derived from the exchange of cis and trans forms at Pro^7–Pro^8. Further study with theoretical modeling revealed that the p3 peptide has a curb conformation without regular secondary structure. On the other hand, the NMR studies for the p3 peptide with the GM1 micelles elucidated a trans conformer and gave a structure stabilized by hydrophobic interactions of β- and helical turns. Based on these structural investigations, tryptophan, a core residue of the hydrophobic cluster, might be an essential residue for the recognition of the GM1 saccharides. The dynamic transition of the p3 peptide may play an important role in the function of GM1 as a multiple receptor as in the traditional pathway of the infection by cholera toxin.

Keywords: Molecular induction; Molecular recognition; GM1; Functional peptide; p3 Peptide

1. Introduction

With the recent success of the human genome analysis, in the life-science research field it is natural to become focused not only on protein structure but also on protein structure–function relationships. Nuclear magnetic resonance spectroscopy is a powerful tool for the study of molecular structures and allows for the analysis of the solution phase structure once the target compound has been dissolved in a suitable deuterated solvent. Unfortunately, the usual target proteins are often too big to study by NMR, which is best for the analysis of proteins smaller than 15 kDa and a maximum of 30 kDa.[1] Although the Kay[2] and Wüthrich[3] groups have reported NMR studies for larger proteins, 723 residues and 900 kDa, respectively, neither was a complete determination. To overcome this problem, designing partially mimetic proteins or the use of part of the protein as the NMR research target has been widely explored, but in many cases the original function is lost due to changes in overall conformation or entropy penalties.

Based on these difficulties, we planned an 'opposite' approach to study protein function, which focuses on 'functional small-module peptides'. We can then study conformational or dynamics details by NMR more easily because the molecular size is small enough for NMR spectroscopy. After elucidation of the binding details, a

* Corresponding authors. Tel.: +81 11 857 8497; fax: +81 11 857 8435 (H.S.); tel.: +81 11 857 8472; fax: +81 11 857 8441 (S.-I.N.); e-mail addresses: hiroki.shimizu@aist.go.jp; shin@glyco.sci.hokudai.ac.jp; tiger.nishimura@aist.go.jp

0008-6215/$ - see front matter © 2007 Elsevier Ltd. All rights reserved.
doi:10.1016/j.carres.2007.05.026

search for identical or similar linear or three-dimensional structures in the Protein Data Bank is carried out. The hit protein will have the same or similar function as the original peptide. Even if we cannot find any similar proteins in the Protein Data Bank, we can design efficiently, based on this knowledge, functional proteins, or so called 'artificial enzymes'.

Gangliosides are neuraminic acid-bearing glycosphingolipids found in eukaryotic cells and are the major sialylated glycoconjugates in the brain.[4] Through their carbohydrate moieties, they are receptors for viral and bacterial toxins, contribute to cell–cell and cell–matrix interactions and regulate cell growth.[5–8] Therefore, it is expected that the elucidation of the mechanism and inhibition of ganglioside–toxin interactions will potentially prevent various diseases.

In a previous study,[9] we presented three types of novel peptides that bind to the pentasaccharide portion of GM1 (β-D-Gal*p*-(1→3)-β-D-Gal*p*NAc-(1→4)(α-D-Neu*p*Ac-(2→3))-β-D-Gal*p*-(1→4)-β-D-Glc*p*-(1→1′)-Cer), which were identified with the improved phage display technique. One, called 'p3', strongly binds to GM1 saccharides with a 1.2 μM dissociation constant by QCM (quartz crystal microbalance).[10] This is the first reported artificial peptide with no homology to any native proteins and peptides with the ability to recognize GM1. The p3 peptide is expected to be an efficient substance for the development of GM1-binding inhibitors as well as an optimal model for clarifying ganglioside–peptide interactions. In this study, using p3, which has the primary sequence VWRLLAPPFSNRLLP, we studied the interaction of the peptide with GM1 oligosaccharide using NMR methods and computational methods.

2. Results

2.1. NMR analysis of the p3 peptide

Well-resolved spectra of p3 were obtained for both conditions (with or without ganglioside GM1) as described in Section 4 and the observed cross-peaks were assigned completely according to the sequence specific assignment of Wüthrich.[11] The identification of spin systems of the amino acids was based on scalar coupling patterns observed in TOCSY experiments, and complemented with ROESY and NOESY measurements. The sequential connectivities were identified by the assignments of distance information, ROEs or NOEs, which are $^{\alpha}$H(i)–NH($i+1$) ($d_{\alpha N}$), $^{\beta}$H(i)–NH($i+1$) ($d_{\beta N}$), and NH(i)-NH($i+1$) (d_{NN}). A summary of the sequential assignments is shown in Figure 1.

In the case of the spectra with p3 alone, it was found that each residue showed two kinds of scalar coupling networks in the TOCSY spectra at the beginning of spectral analyses (Fig. 2). One had strong intensity and

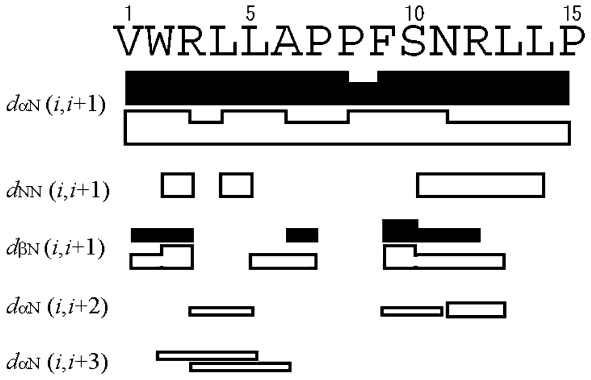

Figure 1. Summary of ROE or NOE connectivities of p3 in the presence and absence of GM1 oligosaccharide. The sequential ROEs and NOEs, $d_{\alpha N}(i,i+1)$, $d_{\beta N}(i,i+1)$ and $d_{NN}(i,i+1)$, and the medium-range NOEs, $d_{\alpha N}(i,i+2)$ and $d_{\alpha N}(i,i+3)$, are represented by bars and classified into strong, medium, weak, and very weak intensities according to the height of the bars. Black bars indicate the ROE connectivities of the peptide in the free state, and white bars represent complex states with GM1 micelles.

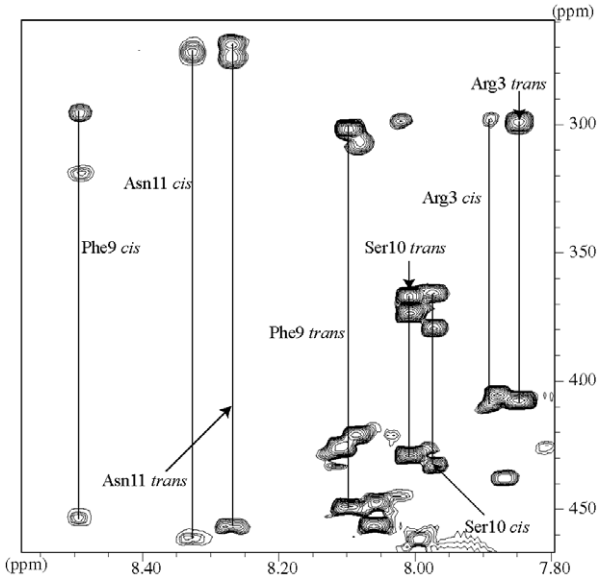

Figure 2. NH-aliphatic region of TOCSY spectrum of the free state of p3. Two different spin systems were detected for each residue. The assignments of Arg^3, Phe^9, Ser^{10}, and Asn^{11} are labeled in this figure. This TOCSY spectrum was recorded with 80 ms of the spin-lock time.

the other was weak, which suggested slow conformational exchange of the protein that occurred in aqueous solution. ROE analyses successfully revealed the details of the coupling networks observed in the TOCSY spectra. In the one with weak intensity, the Pro^7–Pro^8 peptide bond was determined to have cis conformation because the detection of ROE $d_{\alpha\alpha}$ was of stronger intensity than that of $d_{\alpha\delta}$. Another network with strong intensity had a trans conformation in this site. In this solution sample, 114 ROEs for the trans conformer were gathered as distance information for structural calculation although sufficient inter-residual ROEs were not

observed for the *cis* peptide. In this study, we defined a *trans* peptide as a major component of the p3 peptide. As the most impressive information reflecting the structure of this peptide, two long-range ROE between Trp^2εH3 and Leu^{14}βHs, and between Trp^2εH3 and Leu^{14}γH were observed, which suggested that the N- and the C-terminal of the peptide were in close proximity. Whereas the ROEs between hydrophobic side chains (i to $i+1$, i to $i+2$ relations) were observed, other characteristic ROEs for secondary and tertiary structure were not observed. Unfortunately only poor NOESY spectra were obtained, because $\omega\tau_c$ (τ_c: molecular correlation time) of the peptide might become zero depending on the intensity of NOE. Thus, ROESY experiments were used to obtain the proton–proton distance information.

To reveal the structure of this GM1-binding peptide, NMR experiments were carried out with the p3-GM1 complex (p3 peptide 3 mM with GM1 0.3 mM). Because the primary critical micellar concentration of GM1 is 3.32 μM,[12] GM1 under these conditions would form a micelle. The fact that the p3 was found by the QCM method to a GM1 monolayer indicated that the peptide surely interacts with a pentasaccharide region of GM1.[10] Thus, forming a micelle of GM1 was not an improper condition. Moreover, it could be an advantage to avoid nonspecific binding with the ceramide portion of the molecule.

In TOCSY spectra, three kinds of scalar coupling networks were observed, which were derived from the GM1-binding state and the free state of trans and cis conformers. The NOESY experiments gave sufficient signals derived from the complex, though the signals of the free state of p3 were found only with very weak intensity such as NOESY spectra. A total of 146 NOEs could be assigned from complex state NOESY spectra for constraints of structure calculation. As one of the characteristic NOEs, six sequential NOEs between backbone amides, Trp^2–Arg^3, Leu^4–Leu^5, Ser^{10}–Asn^{11}, Asn^{11}–Arg^{12}, Arg^{12}–Leu^{13}, and Leu^{13}–Leu^{14}, were found, whereas no NH–NH NOEs were observed in the spectra of p3 alone (Fig. 3). A total of 28 and 12 new sequential and medium-range NOEs, respectively, were also discovered suggesting that the peptide forms a stable conformation. Furthermore, NOEs derived from the aromatic ring of Trp^2, including long-range interactions, were newly identified (Fig. 4), indicating restriction of Trp^2 mobility in the presence of GM1.

For the samples of p3 alone and the p3–GM1 complex, the $^3J_{HN\alpha}$ were determined by high-resolution DQF–COSY spectra to estimate the restraint of dihedral angle ϕ. In the free state, $^3J_{HN\alpha}$ of Arg^3 was more than 8.0 Hz (dihedral angle ϕ is approximately $-120°$), and Leu^5 and Leu^{14} were less than 6.0 Hz (dihedral angle ϕ is approximately $-60°$). On the other hand, $^3J_{HN\alpha}$ of Trp^2, Leu^5, Ala^6, and Phe^9 were greater than 8.0 Hz, and Arg^3, Asn^{11} and Leu^{12} were less than 6.0 Hz. These results indicate that the conformation of the peptide was changed by the addition of GM1. In particular, Arg^3, Leu^5 and Ala^6 represented a drastically changed dihedral angle ϕ, and the C-terminal region including Asn^{11} and Arg^{12} was predicted by constructing a helical conformation by the combination of dihedral angles and NH–NH NOEs.

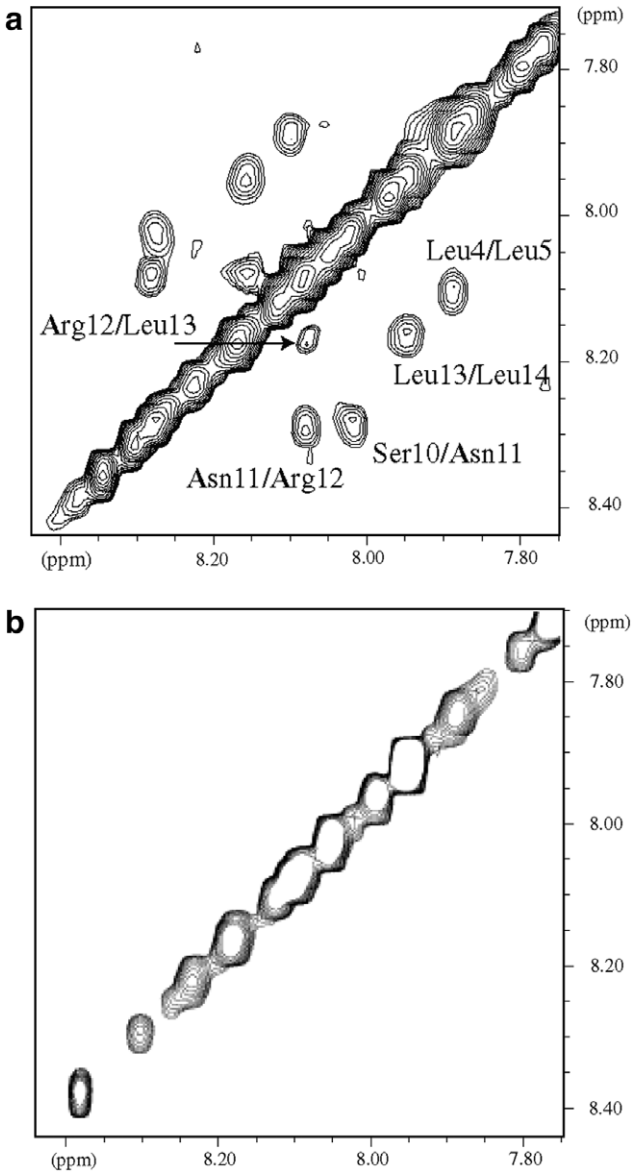

Figure 3. NH–NH region of ROESY and NOESY spectra of p3 in the presence (a) and absence (b) of GM1 oligosaccharide. Sequential NOEs between backbone amides were detected in the complex state with p3 (a), although corresponding ROEs could not be observed in the case of p3 alone (b). Four of six NOEs are shown in (a) with assignment labels. These ROESY and NOESY spectra were performed with 250 ms of mixing time.

2.2. Structure determination by NMR

We carried out the structural calculations with the program CNS 1.1[13] to determine the three-dimensional

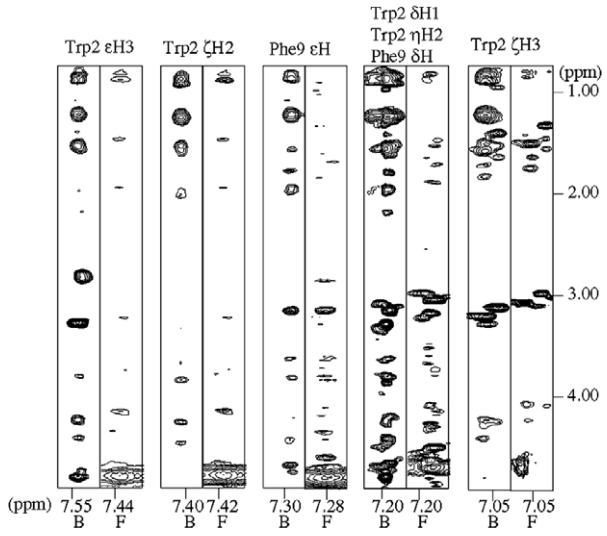

Figure 4. Aromatic–aliphatic regions of ROESY spectra of the p3 alone and NOESY spectra of the p3 with GM1 oligosaccharide. The stripped spectra of the region of aromatic protons are shown to investigate the increment of NOEs led by the addition of GM1. On the top of each strip, the name of the observed aromatic proton and characters B and F in the figure indicate the bound and the free states of p3, respectively.

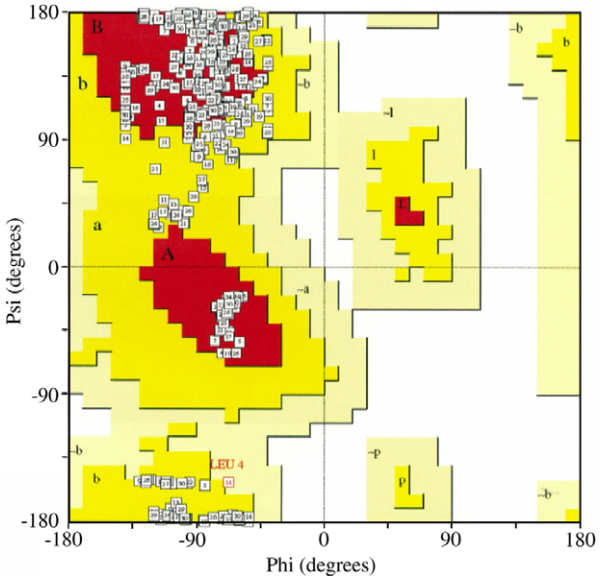

Figure 5. Ramachandran plot of the obtained 30 structures of p3. All residues except for prolines are located on the allowed region, suggesting that p3 has a general structure without irregular conformation.

solution structure of the p3 GM1-binding peptide, in the presence and absence of the GM1 micelle. Calculations were carried out using the 114 and 146 intramolecular ROEs and NOEs as distance constraints in the absence or presence of GM1, respectively. The 114 distance restraints included 66 intraresidue ($|i-j|=0$), 29 sequential ($|i-j|=1$), 17 medium ($2\leqslant|i-j|\leqslant4$), and two long-range ($|i-j|\geqslant5$) ROEs, and the 146 distance constraints included 57 intraresidue ($|i-j|=0$), 57 sequential ($|i-j|=1$), 27 medium ($2\leqslant|i-j|\leqslant4$), and five long-range ($|i-j|\geqslant5$) NOEs. In the first step, the structure calculations were performed without the restraints of dihedral angles, but with only the distance constraints estimated from NOE intensities. Restraints with large violations were removed or modified in this step. In the next step, a total of three and seven dihedral angle ϕ restraints were added for calculation of the p3 peptide alone and the p3–GM1 complex cases, respectively. In the final step, to locate each dihedral angle ϕ on the allowed position in the Ramachandran plot, highly loose constraints $-100\pm80°$ were applied.

Finally, a family of 25 accepted three-dimensional structures were selected with the lowest potential energies that contained no experimental violations greater than 1.0 Å and 1° in the distance and torsion angle restraints, respectively. In the Ramachandran plots shown in Figure 5, 99.7% and 99.3% for the p3 peptide alone and the p3–GM1 complex, respectively, of the backbone dihedral angles of the 25 converged structures fell within the allowed regions. A summary of the energetic statistics for the GM1-binding peptide is shown in Table 1.

Table 1. Structural statistics for p3 in the presence or absence of GM1 micelles

	Absence of GM1	Presence of GM1
Average potential energies (kcal mol^{-1})[a]		
E_{total}	22.81 ± 1.71	32.29 ± 2.88
E_{bonds}	0.46 ± 0.07	1.04 ± 0.18
E_{angle}	14.95 ± 0.23	18.66 ± 1.36
E_{impr}	0.32 ± 0.09	1.14 ± 0.23
E_{VDW}[b]	5.16 ± 1.17	9.78 ± 1.40
E_{NOE}[b]	1.92 ± 0.53	1.90 ± 0.94
E_{cdih}[b]	0.009 ± 0.001	0.11 ± 0.05
RMSD from idealized geometry		
Bonds (Å)	0.0013 ± 0.0001	0.0020 ± 0.0002
Angles (°)	0.4461 ± 0.0035	0.4981 ± 0.0180
Impropers (°)	0.1182 ± 0.0015	0.2250 ± 0.0022
Pairwise RMSD of 25 structures from Val^{1} to Leu^{14} (Å)		
Backbone atoms (N, Cα, C′)	1.31 ± 0.36	0.37 ± 0.11
All heavy atoms	2.52 ± 0.67	1.14 ± 0.21

All energies and RMSD values were calculated using the CNS 1.1[28] and MOLMOL[31] programs, respectively.

[a] E_{impr}, E_{VDW}, E_{NOE}, and E_{cdih} are the energy of improper torsion angles, the van der Waals repulsion energy, the square-well NOE potential energy and the dihedral potential energy, respectively.

[b] The force constants for the calculations of E_{VDW}, E_{NOE}, and E_{cdih} were 4.0 kcal mol^{-1} Å^{-4}, 50 kcal mol^{-1} Å^{-1} and 200 kcal mol^{-1} rad^{-2}, respectively.

Figure 6 shows the structures of p3 in the presence and absence of GM1 oligosaccharide. For the p3 without GM1, the pairwise RMSD values for the 25 lowest-energy structures were found to be 1.31 ± 0.36 Å for backbone atoms and 2.52 ± 0.67 Å for all heavy

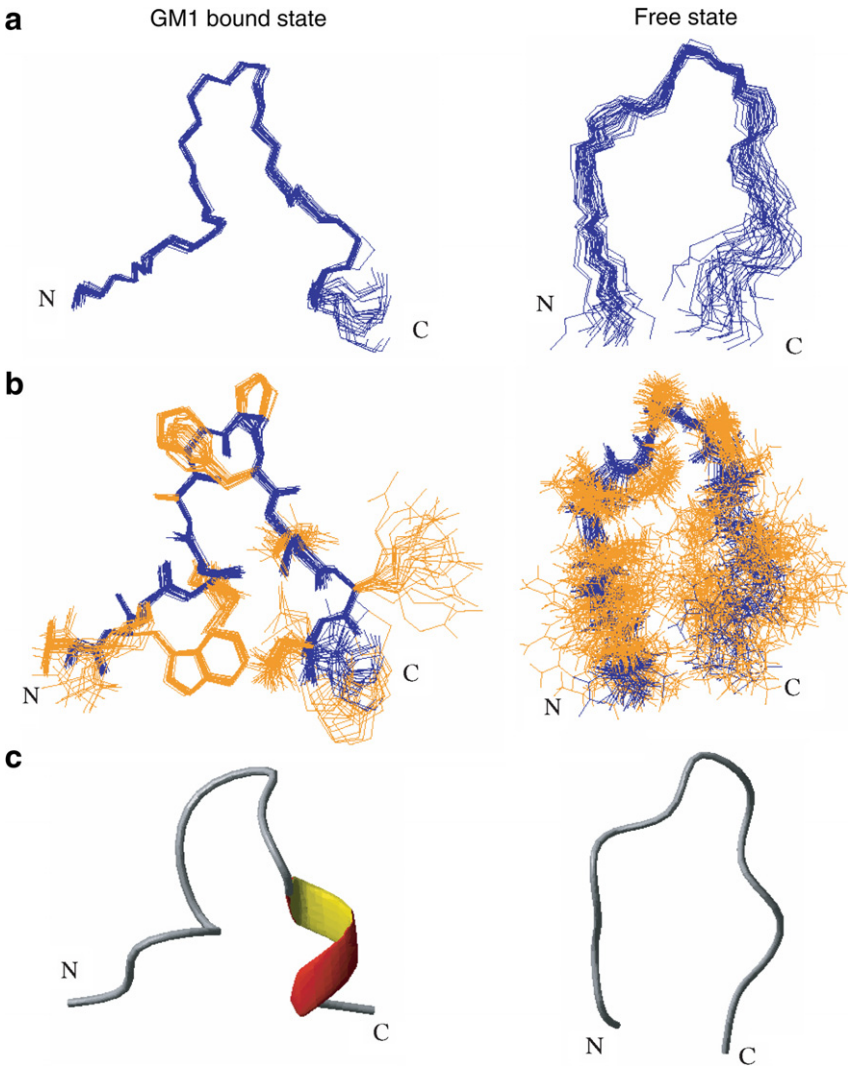

Figure 6. Three-dimensional structures of p3. Twenty five structures are superimposed to the backbone atoms from Val[1] to Leu[14]. The structures of p3 in the presence and absence of GM1 micelles are displayed in the left and right columns, respectively. (a) and (b) represent structures of the backbone atoms and all heavy atoms including side chains, respectively. Blue and orange lines indicate the backbone and side chains, respectively. (c) is the lowest-energy models of 25 structures. This figure was generated by MOLMOL[33] software.

atoms when the structures were fit in the region of Val[1]–Leu[14]. From the NMR data, p3 without GM1 formed a curb at the middle and had variable conformation without regular secondary structure. This peptide, however, had the specific conformations in local areas, for example, Val[1]–Ala[6] and Pro[7]–Arg[12], with 0.46 ± 0.15 and 0.58 ± 0.18 Å of the RMSD value of backbone atoms, respectively. Hydrophobic interactions stabilized the conformations of both regions. The region from Val[1] to Ala[6] had a hydrophobic surface constructed to the side chains of Trp[2], Leu[4], and Leu[5] and the region from Pro[7] to Arg[12] formed a rigid turn with the hydrophobic contacts of proline rings and the aromatic ring of Phe[9].

On the other hand, the greatly converged structure of the peptide in the presence of GM1 micelle was determined to have RMSD values of 0.37 ± 0.11 and 1.14 ± 0.21 Å for the backbone atoms and all heavy atoms, respectively. The fluctuation of the peptide was reduced significantly compared to the peptide alone. The 25 lowest-energy structures in the region of Val[1]–Leu[14] are superimposed in Figure 6. The molecule maintained the bent structure with the rigid turn made by the Pro[7]–Pro[8] portion. The most noteworthy feature of this structure is the hydrophobic cluster, including Trp[2], Leu[4], Leu[5], Leu[13], and Leu[14]. The residues forming a hydrophobic surface, Trp[2], Leu[4], and Leu[5] in the case of the structure absent from GM1, are toward the inside of the peptide, and the aromatic ring of Trp[2] is surrounded by the N- and C-terminal leucines. Moreover, two stable turns were found in the regions of Trp[2]–Leu[5] and Ser[10]–Arg[12]. The former was identified as a β-turn using the standard criterion with the distance between $^{\alpha}C(i)$ and $^{\alpha}C(i+3)$ as less than 7 Å.[13] The average distance between $^{\alpha}C$ atoms of Trp[2] and Leu[5]

was 5.35 Å. This turn had a nearly type I β-turn conformation from the viewpoint of the dihedral angles of constructing residues. However, no NMR information about the hydrogen bonding was obtained, and furthermore it was clarified that there was no intra-turn hydrogen bond in the calculated structures. This turn was therefore defined as a $\beta_E\gamma$-type turn,[14] that is, a type-IV β-turn (miscellaneous type) according to the classical nomenclature. The second turn was a helical turn like the conformation of the 3_{10} helix. The C-terminal region of p3 showed a highly disordered structure absent from GM1, therefore this region might play an important role in binding to GM1 saccharides.

2.3. Molecular dynamics study for the p3

Molecular dynamics (MD) simulations were also carried out. Two major structures were obtained with the MD calculations within 40 ns at 325 K, preceded by the MD to generate the starting geometries at high temperature. These were in good agreement with the fluctuating conformations obtained by NMR experiments. One of these had a curb form at the middle of p^3, Pro^7–Phe^9, and there were no characteristic hydrogen bonds in half of the N-terminus, which meant that the peptide did not have a specific secondary structure (Fig. 7). Although the RMSD between the structures from the NMR study and the MD simulation was large (4.67 Å), both structures had the same topology. This suggested that the MD simulations were able to support the NMR experiments. Figure 8 shows the other structure obtained by MD with the bound p3 NMR backbone structure. Although we have not considered the existence of GM1 during these simulations, we found that the RMSD for the backbone structure of 3.56 Å was smaller than the case in Figure 8.

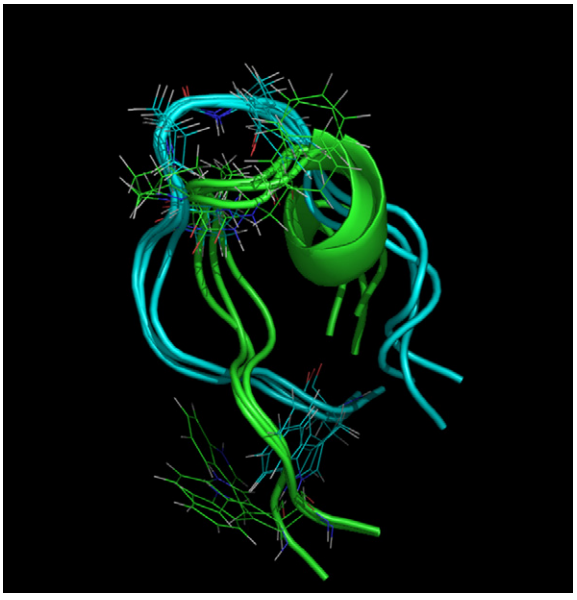

Figure 7. Superimposed structure of p3 from MD simulations (green) and from NMR data without GM1. Both have the same topologies including (i) curb structure at the middle and (ii) no secondary structure although MD simulation showed 'helix-like' predicted structure at the C-terminal area. Side chains of key residues that bind GM1, Pro^7–Phe^9 and Trp^2, are also shown.

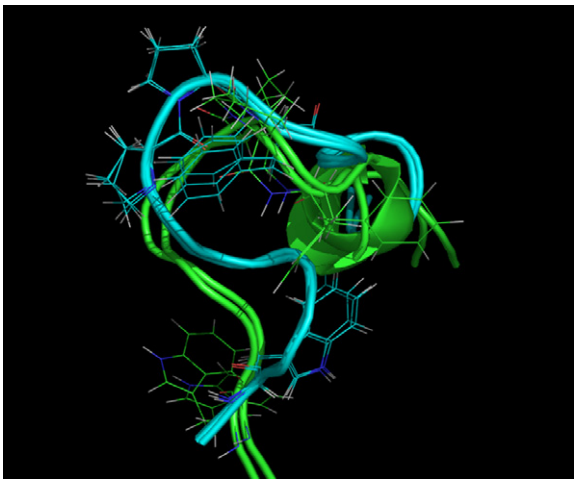

Figure 8. Superimposed structure of p3 from MD simulations (green) and from NMR data with GM1. Although the MD calculations were performed without any ligand, the structure from MD was similar to the structure from NMR with GM1. Side chains of key residues that bind GM1, Pro^7–Phe^9 and Trp^2, are also shown.

3. Discussion

In summary, the structure of the p3 peptide was stabilized completely in the presence of the GM1 oligosaccharide, which existed in the micelle form. In the bound form, the peptide is stabilized by forming stable β- and helical turns, whereas the Pro^7–Pro^8 region contributing to the bend in the peptide structure was preserved.[15,16] Therefore, it can be suggested that the N- and the C-terminal regions underwent drastic conformational change upon the binding of the GM1 pentasaccharide (Fig. 6). Unfortunately, no characteristic intermolecular NOEs that could suggest a specific binding site were observed in this study because GM1 formed micelles in aqueous solution and thus gave significant line-broadening in the NMR spectra.

Previous studies on lectins proposed that the modular structure of the aromatic ring of tryptophan on the β-turn, known as the carbohydrate-binding module (CBM), plays a key role in the hydrophobic interaction with the nonpolar face of monosaccharide rings.[17–19] Based on the structural analyses of p3, Trp^2 of the bound state was also included in the β-turn and constructed a hydrophobic core. We, therefore, propose that Trp^2 would be an essential residue for binding to

GM1 pentasaccharide. Moreover, for the representative example of the recognition of NeuAc, arginine binds to the carboxyl group of NeuAc through the electrostatic interaction in the coat protein of murine polyoma virus.[20] This GM1-binding peptide had two arginines, Arg^3 and Arg^{12}, located on the β-turn and the helical turn, respectively. From the viewpoint of the solution structure of the bound state, the side chain of Arg^{12} was exposed to solvent with more disordered direction than that of Arg^3, which would suggest that Arg^3 is strongly involved in the recognition of NeuAc in GM1.

Although Honda et al. reported the conformation of a 10 amino acid residual peptide,[21] it is difficult, in general, for a small peptide to form a steady conformation and create a stable binding site for oligosaccharides in aqueous solution. Thus our results indicate that the structure of ligand peptide was controlled by the carbohydrate platform. Whereas it is frequently reported that gangliosides on the cell surface behave as receptors to various ligands, we believe that the regulation of the protein and peptide structure is also one of the most essential functions of carbohydrates. As another interesting study on ganglioside–peptide interaction, it has also been reported that enkephalins, endogenous neurotransmitters consisting of five amino acids have altered folding in the bound state with GM1 micelle.[22] This study indicated that enkephalins had an induced rigid turn structure by interaction with the GM1 micelle, which was very similar with the structure in bicelles.[23] Moreover, the nonapeptide bradykinin, a neuropeptide with an antiphlogistic effect, was also recently confirmed to undergo conformational change on binding to GM1 micelles.[24] These drastic transitions of the structure of ligand peptide on GM1 surface are likely to play an important role in the ignition of sequential events like the traditional pathway of cholera toxin infection.

4. Experimental

4.1. General

Unless otherwise stated, all commercially available solvents and reagents were used without further purification. Fmoc amino acid derivatives and resin were purchased from NOVA Biochem Co. Ltd. Automatic peptide synthesis was performed with Advanced Chem Tech MODEL Apex396 peptide synthesizer. HPLC was performed on a Hitachi HPLC system equipped with an L-7150 intelligent pump, an L-7420 UV detector and reversed-phase C18 column, Inertsil® ODS-3 (20×250 mm) at a flow rate of 5.0 mL min^{-1}. The eluate was monitored by UV absorption at 220 nm. MALDI-TOF MS analyses were performed with the Bruker REFLEXIII mass spectrometry with 2,5-dihydroxybenzoic acid (DHB).

4.2. Preparation of samples

GM1 was purchased from Wako Pure Chemical Industries, Ltd. (Osaka, Japan) and was used without further purification.

The p3 peptide, VWRLLAPPFSNRLLP,[9,10] was synthesized on Fmoc-Pro-OH preloaded 2-chlorotrityl chloride resin (0.66 mmol/g) using an automatic peptide synthesizer (a common solid-phase peptide synthetic method with Fmoc strategy) in four batches on 0.02 mmol scale each (four portions of 30 mg of preloaded resin each). Fmoc amino acid derivatives, Fmoc-Pro-OH, Fmoc-Leu-OH, Fmoc-Arg(Pbf)-OH, Fmoc-Asn(Trt)-OH, Fmoc-Ser(*t*Bu)-OH, Fmoc-Phe-OH, Fmoc-Ala-OH, Fmoc-Trp(Boc)-OH and Fmoc-Val-OH, were employed. A cycle of automated peptide synthesizer for a 0.02 mmol scale was defined as follows. The resin was treated with 1.5 mL of 20% (v/v) piperidine in DMF and the mixture was stirred for 5 min at ambient temperature. After filtration, the same process was performed but stirred for 15 min. Then, the resin was washed with NMP (*N*-methylpyrrolidine, 1.5 mL) and DMF (1.5 mL). To a mixture of a solution of Fmoc amino acid (4 equiv) and HOBt (*N*-hydroxybenzotriazole, 3.5 equiv) in NMP (600 μL) and a solution of HBTU (2-(1*H*-benzotriazole-1-yl)-1,1,3,3-tetramethyluronium hexafluorophosphate, 4 equiv) and DIEA (diisopropylethylamine, 6 equiv) in DMF (600 μL) was added the resin, and the reaction mixture was stirred for 40 min at ambient temperature. This coupling process was performed twice. After washing the resin with NMP (1.5 mL) and DMF (1.5 mL), nonreactive amino groups were acetyl-capped with 1.5 mL of a mixed solution of Ac_2O (4.75% as v/v) and HOBt (13 mM) in NMP. After completing the peptide synthesis process, the resin was washed with NMP (1.5 mL) and CH_2Cl_2 (1.5 mL), and dried in vacuo. The protected peptide on the resin was treated with 10 mL of a mixed solution of TFA/H_2O/ethanedithiol/triisopropylsilane (94.5/2.5/2.5/1.0 (v/v/v/v)) for 3 h at ambient temperature followed by washing with TFA (2 mL) to remove the peptide from resin and for deprotection of protecting groups such as -*t*Bu, -Trt, -Pbf, and -Boc. The combined solvent was dried with blowing N_2 gas and precipitated from cold dry *tert*-butylmethyl ether. The obtained white solid was purified by HPLC [eluate: solvent A (0.1% TFA in H_2O) and solvent B (0.1% TFA in acetonitrile), gradient; increase from 2% to 60% of B over 60 min]. The fractions containing the desired peptide were collected and lyophilized. The p3 peptide was obtained as a white powder (72 mg, 50% overall yield). Typical NMR data are shown in the figures. Amino acid analysis (theoretical ratio): Asp (Asn) 1.0 (1), Ser 0.8 (1), Ala 1.0 (1), Val 0.9 (1), Leu 4.0 (4), Phe 1.0 (1), Trp 0.9 (1), Arg 2.1 (2); MALDI-TOF-MS calcd for $[M+H]^+$ 1779.043, found $[M+H]^+$ 1779.827.

4.3. NMR measurements

Sample solutions for NMR measurements were prepared by dissolving p3 in a mixed solvent of 10% D_2O, 90% H_2O or 99.9% D_2O, and the sample pH was adjusted to 4.1. All NMR spectra were measured on a Bruker Avance 600 spectrometer equipped with a cryoprobe system operating at 600.13 MHz for the proton frequency. The sample was not spun and the spectra were recorded at a temperature of 300 K. Data acquisition was performed with XWINNMR 3.1 (Bruker) software operating on a Silicon Graphics O2+ workstation. The water signal was suppressed by low-power irradiation during the relaxation delay time and WATERGATE method with 3–9–19 pulse sequence with *x*, *y*, *z*-triple gradient.[25,26] One-dimensional ^{1}H NMR experiments were performed with a spectral width of 6009.615 Hz, 32K data points and 8 scans. Two-dimensional DQF–COSY,[27] TOCSY,[28,29] ROESY,[30] and NOESY[31] measurements were recorded in a phase sensitive mode. The TOCSY transfer was achieved with the MLEV-17 pulse sequence with spin-locking times of 60, 80, and 100 ms. ROESY and NOESY spectra were recorded with mixing times of 150 and 250 ms, respectively. Except for DQF–COSY determination of the $^3J_{HN\alpha}$, all two-dimensional measurements were recorded with 2048×512 frequency data points and zero-filled to yield 2048×2048 data matrices. High-resolution DQF–COSY experiments were measured with 4096×512 points and zero-filled to a 8192×8192 matrix with a 0.73 Hz point resolution. The number of scans for all spectra was 8. The time domain data in both dimensions were multiplied by a sine bell window function with 90° phase shift prior to Fourier transformation. All NMR spectra were processed by software NMRPIPE,[32] and the signals were assigned with the XEASY[33] program on a Silicon Graphics O2 workstation.

4.4. Structure modeling based on NMR data

Three-dimensional structures of p3 were calculated with CNS 1.1[34] program on a Linux workstation. A total of 114 and 146 distance restraints for p3 and the complex of the p3 and GM1 samples, respectively, were used to calculate the family of structures. Moreover, 12 dihedral angle ϕ restraints were used for both sample calculations. Distance restraints for calculations were estimated from the cross-peak intensities in ROESY or NOESY spectra with a mixing time of 150 ms; the estimated restraints were then classified as strong, medium, weak, and very weak, and assigned upper limits of 2.7, 3.5, 5.0, and 6.0 Å, respectively. Pseudo-atom corrections were used for unresolved NOE cross-peaks, methyl protons as well as nonstereospecifically assigned methylene and aromatic protons. In addition, 0.5 Å was added to the upper limit of the distance constraints of only the involved methyl protons according to the report by Clore et al.[35] The restraints of the dihedral angle ϕ were based on $^3J_{HN\alpha}$ coupling constants measured in high-resolution DQF–COSY. For checking of the restraints violation, the PROCHEK-NMR 3.5.4[36] program was used on a Linux workstation, and superimposition of the obtained structures, calculation of RMSD values, and general analyses of GM1-binding peptide were performed with MOLMOL[37] software.

4.5. Ab initio computational structural analysis with molecular dynamics simulation

A molecular dynamics simulation was performed with the AMBER software package version 8.0, using the third-generation point-charge all-atom force field for proteins, also known as ff03.[38] The solvents were implicitly represented by a generalized Born solvent model[39] with no cutoff. p3 was constructed with an extended feature using SYBYL Version 6.9 (Tripos Association, St. Louis, MO).

To generate a variety of conformations of p3 as a starting geometry, 500 steps of a molecular dynamics calculation at 900 K with 2 fs time steps were performed. For all structures, the temperature was gradually lowered until the RMS of the Cartesian elements of the gradient was <0.4 kcal/mol Å. Six groups of conformations were obtained and applied in additional MD calculations. Using each conformer as the starting structures, the 40 ns MD with Berendsen's algorithm[40] was carried out. The temperature and the pressures were kept at 325 K and 1 atm, respectively. In this simulation, the integration time step was 2.0 fs, and SHAKE[41] was applied to constrain all bonds connecting hydrogen atoms. The trajectories were saved every 5.0 ps. A total of 48,000 snapshots were sampled and two major conformers were obtained by a cluster analysis,[42] which are shown in Figures 7 and 8. AMBER 8.0 and PROCHECK were used to analyze the trajectories, and simulations were performed on HP GS1280, Sun Fire 12K, IBM p690, and a Linux cluster with 12 Pentium IV (2 GHz) CPUs.

Acknowledgments

The authors thank Professor Jesús Jiménz-Barbero, Centro de Investigaciones Biologicas, Madrid, Spain, for providing the opportunity to participate in this special issue of Carbohydrate Research on Glycomimetics, and Dr. Nobuaki Nemoto, JEOL Ltd., Akishima, Japan, for useful discussion.

References

1. Gabius, H.-J.; Siebert, H.-C.; André, S.; Jiménez-Barbero, J.; Rüdiger, H. *ChemBioChem* **2004**, *5*, 740–764.

2. Tugarinov, V.; Muhandiram, R.; Ayed, A.; Kay, L. E. *J. Am. Chem. Soc.* **2002**, *124*, 10025–10035.
3. Fiaux, J.; Bertelsen, E. B.; Horwich, A. L.; Wüthrich, K. *Nature* **2002**, *418*, 207–211.
4. Vyas, A. A.; Schnaar, R. L. *Biochimie* **2001**, *83*, 677–682.
5. Lloyd, K. O.; Furukawa, K. *Glycoconjugate J.* **1998**, *15*, 627–636.
6. Suzuki, Y. *Prog. Lipid Res.* **1994**, *33*, 429–457.
7. Hakomori, S. *Annu. Rev. Biochem.* **1981**, *50*, 733–764.
8. Iwabuchi, K.; Yamamura, S.; Prenetti, A.; Handa, K.; Hakomori, S. *J. Biol. Chem.* **1998**, *273*, 9130–9138.
9. Matsubara, T.; Ishikawa, D.; Taki, T.; Okahata, Y.; Sato, T. *FEBS Lett.* **1999**, *456*, 253–256.
10. Matsubara, T.; Iijima, K.; Nakamura, M.; Taki, T.; Okahata, Y.; Sato, T. *Langmuir* **2007**, *23*, 708–714.
11. Wüthrich, K. *NMR of Proteins and Nucleic Acids*; John Wiley and Sons: New York, 1986.
12. Basu, A.; Glew, R. H. *J. Biol. Chem.* **1985**, *260*, 13067–13073.
13. Lewis, P. N.; Momany, F. A.; Scheraga, H. A. *Biochim. Biophys. Acta* **1973**, *303*, 211–229.
14. Wilmot, C. M.; Thornton, J. M. *Protein Eng.* **1990**, *3*, 479–493.
15. Espinosa, J. F.; Gellman, S. H. *Angew. Chem., Int. Ed.* **2000**, *39*, 2330–2333.
16. Aemissegger, A.; Kräutler, V.; van Gunsteren, W. F.; Hilvert, D. *J. Am. Chem. Soc.* **2005**, *127*, 2929–2936.
17. Tormo, J.; Lamed, R.; Chirino, A. J.; Morag, E.; Bayer, E. A.; Shoham, Y.; Steitz, T. A. *EMBO J.* **1996**, *15*, 5739–5751.
18. Din, N.; Forsythe, I. J.; Burntnick, L. D.; Gilkes, N. R.; Miller, R. C., Jr.; Warren, R. A.; Kilburn, D. G. *Mol. Microbiol.* **1994**, *11*, 747–755.
19. Nagy, T.; Simpson, P. J.; Williamson, M. P.; Hazlewood, G. P.; Gilbert, H. J.; Orosz, T. A. *FEBS Lett.* **1998**, *429*, 312–316.
20. Stehle, T.; Yan, Y.; Benjamin, T. L.; Harrison, S. C. *Nature* **1994**, *369*, 160–163.
21. Honda, S.; Yamasaki, K.; Sawada, Y.; Morii, H. *Structure* **2004**, *12*, 1507–1518.
22. Chatterjee, C.; Mukhopadhyay, C. *Biopolymers* **2003**, *70*, 512–521.
23. Marcotte, I.; Separovic, F.; Auger, M.; Gagné, S. M. *Biophys. J.* **2004**, *86*, 1587–1600.
24. Chatterjee, C.; Mukhopadhyay, C. *Biochem. Biophys. Res. Commun.* **2004**, *315*, 866–871.
25. Piotto, M.; Saudek, V.; Sklenář, V. *J. Biomol. NMR* **1992**, *2*, 661–666.
26. Sklenár, V.; Piotto, M.; Leppik, R.; Saudek, V. *J. Magn. Reson. A* **1993**, *102*, 241–245.
27. Rance, M.; Sørensen, O. W.; Bodenhausen, G.; Wagner, G.; Ernst, R. R.; Wüthrich, K. *Biochem. Biophys. Res. Commun.* **1983**, *117*, 479–485.
28. Braunschweiler, L.; Ernst, R. R. *J. Magn. Reson.* **1983**, *53*, 521–528.
29. Bax, A.; Davis, D. G. *J. Magn. Reson.* **1985**, *65*, 355–360.
30. Bothner-By, A. A.; Stephens, R. L.; Lee, J.-M.; Warren, C. D.; Jeanloz, R. W. *J. Am. Chem. Soc.* **1984**, *106*, 811–813.
31. Jeener, J.; Meier, B. N.; Bachmann, P.; Ernst, R. R. *J. Chem. Phys.* **1979**, *71*, 4546–4553.
32. Delaglio, F.; Grzesiek, S.; Vuister, G.; Zhu, G.; Pfeifer, J.; Bax, A. *J. Biomol. NMR* **1995**, *6*, 277–293.
33. Bartels, C.; Xia, T. H.; Billeter, M.; Güntert, P.; Wüthrich, K. *J. Biomol. NMR* **1995**, *6*, 1–10.
34. Brünger, A. T.; Adams, P. D.; Clore, G. M.; DeLano, W. L.; Gros, P.; Grosse-Kunstleve, R. W.; Jiang, J.-S.; Kuszewski, J.; Nilges, M.; Pannu, N.; Read, R. J.; Rice, L. M.; Simonson, T.; Warren, G. L. *Acta Crystallogr., Sect. D* **1998**, *54*, 905–921.
35. Clore, G. M.; Gronenborn, A. M.; Nilges, M.; Ryan, C. A. *Biochemistry* **1987**, *26*, 8012–8023.
36. Laskowski, R. A.; Rullmann, J. A. C.; MacArthur, M. W.; Kaptein, R.; Thornton, J. M. *J. Biomol. NMR* **1996**, *8*, 477–486.
37. Koradi, R.; Billeter, M.; Wüthrich, K. *J. Mol. Graph.* **1996**, *14*, 51–55.
38. Duan, Y.; Wu, C.; Chowdhury, S.; Lee, M. C.; Xiong, G.; Zhang, W.; Yang, R.; Cieplak, P.; Luo, R.; Lee, T.; Caldwell, J.; Wang, J.; Kollman, P. *J. Comput. Chem.* **2003**, *24*, 1999–2012.
39. Onufriev, A.; Bashford, D.; Case, D. A. *Proteins: Struct. Funct. Bioinf.* **2004**, *55*, 383–394.
40. Berendsen, H. J. C.; Postma, J. P. M.; van Gunsteren, W. F.; DiNola, A.; Haak, J. R. *J. Chem. Phys.* **1984**, *81*, 3684–3690.
41. Ryckaert, J.-P.; Ciccotti, G.; Berendsen, H. J. C. *J. Comput. Phys.* **1977**, *23*, 327–341.
42. Jang, S.; Kim, E.; Shin, S.; Pak, Y. *J. Am. Chem. Soc.* **2003**, *125*, 14841–14846.